

OPEN ACCESS

EDITED BY

Alok Agrawal,
Retired, Johnson City, United States

REVIEWED BY

Chunxiong Zheng,
South China Normal University, China
Eknath Kole,
Kavayitri Bahinabai Chaudhari North
Maharashtra University, India

*CORRESPONDENCE

Linghui Pan
✉ panlinghui@gxmu.edu.cn

†These authors have contributed equally to this work

RECEIVED 26 May 2025

ACCEPTED 23 June 2025

PUBLISHED 10 July 2025

CITATION

Jing R, Liao X, Mo J, He S, Xie X, Hu Z and Pan L (2025) Spatiotemporal regulation of ventilator lung injury resolution by TGF- β 1+ regulatory B cells via macrophage vesicle-nanotherapeutics.
Front. Immunol. 16:1635178.
doi: 10.3389/fimmu.2025.1635178

COPYRIGHT

© 2025 Jing, Liao, Mo, He, Xie, Hu and Pan.
This is an open-access article distributed under the terms of the [Creative Commons Attribution License \(CC BY\)](https://creativecommons.org/licenses/by/4.0/). The use, distribution or reproduction in other forums is permitted, provided the original author(s) and the copyright owner(s) are credited and that the original publication in this journal is cited, in accordance with accepted academic practice. No use, distribution or reproduction is permitted which does not comply with these terms.

Spatiotemporal regulation of ventilator lung injury resolution by TGF- β 1+ regulatory B cells via macrophage vesicle-nanotherapeutics

Ren Jing^{1,2†}, Xiaoting Liao^{1,3,4,5†}, Jianlan Mo^{6†}, Sheng He⁷, Xianlong Xie⁸, Zhaokun Hu^{1,3,4,5} and Linghui Pan^{1,3,4,5*}

¹Guangxi Clinical Research Center for Anesthesiology, Guangxi Medical University Cancer Hospital, Nanning, China, ²Department of Breast and Thyroid Surgery, South China Hospital, Medical School, Shenzhen University, Shenzhen, China, ³Department of Anesthesiology, Guangxi Medical University Cancer Hospital, Nanning, China, ⁴Guangxi Engineering Research Center for Tissue & Organ Injury and Repair Medicine, Guangxi Medical University Cancer Hospital, Nanning, China, ⁵Guangxi Key Laboratory for Basic Science and Prevention of Perioperative Organ Dysfunction, Guangxi Medical University Cancer Hospital, Nanning, China, ⁶Department of Anesthesiology, Guangxi Maternal and Child Health Hospital, Nanning, China, ⁷The First Affiliated Hospital, Department of Anesthesiology, Hengyang Medical School, University of South China, Hengyang, Hunan, China, ⁸Department of Intensive Care Unit, Guangxi Medical University Cancer Hospital, Nanning, China

Background: Regulatory B cells (Breg) critically orchestrate inflammatory resolution and tissue repair. This study investigates the therapeutic potential of transforming growth factor (TGF)- β 1-producing Bregs in ventilator-induced lung injury (VILI), leveraging biomimetic nanotechnology to overcome limitations of conventional cytokine delivery.

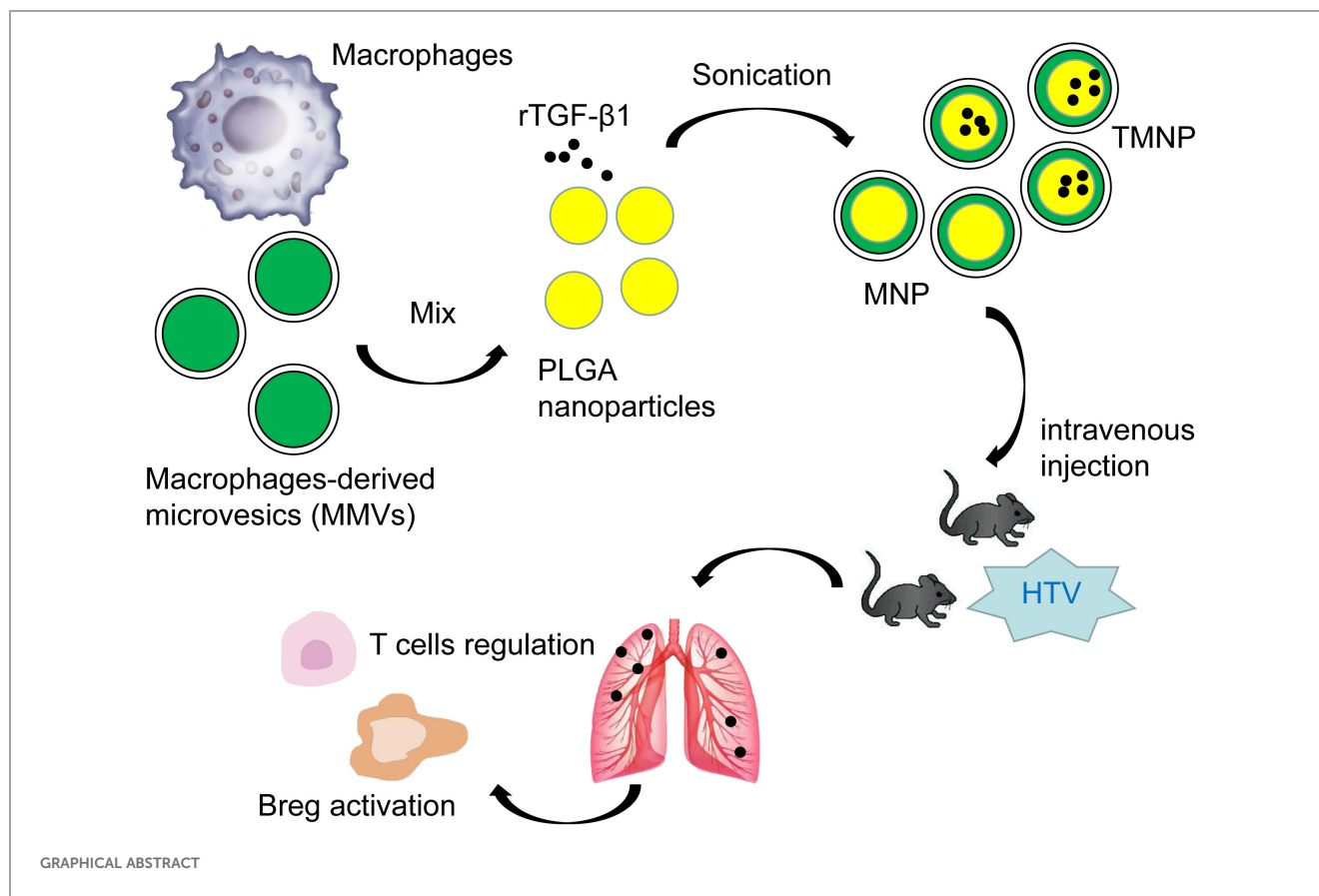
Methods: We engineered macrophage-derived microvesicle-encapsulated nanoparticles (TMNP) for pH-responsive, spatiotemporally controlled TGF- β 1 release. Therapeutic efficacy was evaluated in a murine VILI model through longitudinal immunophenotyping, histopathology, and cytokine profiling at post-ventilation days 1 and 10 (PV1d, PV10d).

Results: VILI triggered biphasic pulmonary Breg expansion (PV1d: 7.83-fold vs. controls, $P < 0.001$; PV10d resurgence) coinciding with peak injury. TMNP administration induced sustained TGF- β 1 bioavailability (PV10d: 3.6-fold vs. free cytokine, $P < 0.001$), attenuating histopathology (22.5% reduction in alveolar hemorrhage, $P < 0.01$) and suppressing IL-6/TNF- α ($P < 0.01$). Treatment concomitantly expanded Breg populations and modulated T cell subset.

Conclusion: TMNP orchestrates Breg-mediated immunoresolution through precision cytokine delivery and lymphocyte modulation, enabling dual-phase protection against ventilation-associated immunopathology. This paradigm represents a transformative approach for acute respiratory distress management.

KEYWORDS

ventilation-induced lung injury, transforming growth factor- β 1, regulatory B cells, immunoresolution, nanoparticles



1 Introduction

Acute lung injury (ALI) and its severe manifestation, acute respiratory distress syndrome (ARDS), constitute life-threatening conditions exacerbated by global health crises like COVID-19 (1, 2). Mechanical ventilation, while essential for ARDS management, paradoxically induces ventilator-induced lung injury (VILI) through synergistic biomechanical forces and inflammatory

Abbreviations: AEC-II, type II alveolar epithelial cells; ALI, acute lung injury; APC, allophycocyanin; ARDS, acute respiratory distress syndrome; BALF, bronchoalveolar lavage fluid; BB515, Brilliant™ Blue 515; Breg, regulatory B cells; CD, cluster of differentiation; CX3CR1, C-X3-C Motif Chemokine Receptor 1; DLC, drug loading capacity; DAPI, 4', 6-diamidino-2-phenylindole; DMEM, dulbecco's modified eagle medium; EE, encapsulation efficiency; ELISA, enzyme linked immunosorbent assay; EOv, end of ventilation; FBS, fetal bovine serum; FITC, fluorescein isothiocyanate; HTV, high tidal volume; HEPES, 4-(2-hydroxyethyl) piperazine-1-erhanesulfonic acid; IL, interleukin; MMVs, macrophage-derived microvesicles; MNP, MMVs membrane-coated nanoparticles; NTV, normal tidal volume; PBS, phosphate buffer saline; PE, P-phycoerythrin; PE/Cy7, PE-Cyanine7; PV1d, post-ventilation one day; PV10d, post-ventilation ten days; rTGF-β1, recombinant mouse TGF-β1; TEM, transmission electron microscope; TGF-β1, transforming growth factor-β1; TMNP, MNP to package TGF-β1; TNF, tumor necrosis factor; Treg, regulatory T cells; VILI, ventilator-induced lung injury.

cascades that disrupt alveolar-capillary integrity (3, 4). Despite lung-protective ventilation strategies, the immunological mechanisms governing injury resolution remain poorly defined, impeding targeted therapeutic development.

Regulatory B cells (Bregs) represent a pivotal immunomodulatory axis that coordinates inflammatory resolution via cytokine secretion (e.g., transforming growth factor [TGF]-β1) and lymphocyte modulation (5, 6). Although Bregs attenuate inflammation in autoimmune and infectious contexts (7–9), their spatiotemporal dynamics and TGF-β1-mediated functions in VILI remain uncharacterized. This knowledge gap persists despite TGF-β1's documented role in mitigating ALI and directing macrophage polarization toward reparative phenotypes (10–12). Crucially, TGF-β1's therapeutic potential is limited by its transient bioavailability ($t_{1/2} \approx 2$ min *in vivo*) (13, 14), necessitating innovative delivery platforms.

To address these critical limitations, we engineered macrophage-derived microvesicles (MMVs)-camouflaged nanoparticles (TMNP) encapsulating TGF-β1-loaded Carboxy-terminated poly(lactic-co-glycolic acid) (PLGA) cores—a biomimetic platform leveraging MMVs' inherent macrophage tropism for targeted alveolar delivery, pH-responsive release kinetics to overcome cytokine instability, and synergistic immunomodulatory properties. Our study specifically interrogates the unexplored role of TGF-β1⁺Bregs in VILI pathogenesis, TMNP's capacity to sustain TGF-β1 bioavailability, and mechanisms underlying Breg-mediated immunoresolution.

2 Materials and methods

2.1 Reagents and chemicals

PLGA (50:50 lactide:glycolide ratio, MW 38–54 kDa, LACTEL B6013-2) served as the polymer matrix. Recombinant mouse TGF- β 1 (BioLegend 763102), cytochalasin B (Abcam ab143482), and uranyl acetate (Sigma-Aldrich 73943) were utilized. All solvents including chloroform (HPLC grade, Sigma-Aldrich 650498) and dimethyl sulfoxide (DMSO, ThermoFisher D12345) met analytical standards.

2.2 Animal subjects

Male C57BL/6 mice (4–6 weeks, 25 ± 5 g) from Guangxi Medical University's Animal Center (Nanning, China) were maintained under specific pathogen-free conditions. All procedures complied with China's Laboratory Animal Welfare Guidelines under IACUC protocol KY-2022-288.

2.3 MMVs isolation

RAW 264.7 macrophages (Cell Bank of Chinese Academy of Sciences) were cultured in advanced Dulbecco's Modified Eagle Medium (DMEM; Gibco, 12491015) supplemented with 10% fetal bovine serum (Gibco, 10270106) and 1% penicillin/streptomycin (Gibco, 15140122). MMVs were generated via cytochalasin B-induced membrane blebbing (15): cells were treated with 10 μ g/ml cytochalasin B in serum-free DMEM for 1 h at 37°C. Following membrane detachment, suspensions underwent sequential centrifugation (5,000 \times g, 10 min; 17,000 \times g, 15 min) with ethylenediaminetetraacetic acid-containing MilliQ washes. Microvesicle protein content was quantified via BCA assay (ThermoFisher, 23227) and validated through CD9/CD63 immunoblotting.

2.4 Nanoparticle synthesis

2.4.1 PLGA core fabrication

Carboxy-terminated PLGA dissolved in chloroform (20 mg/ml) was emulsified with 2.5 μ g recombinant mouse TGF- β 1 using a water-in-oil-in-water double emulsion technique (15). Primary emulsions were sonicated (BILON-1000Y probe sonicator, 60% amplitude, 10-s pulses on ice bath) and introduced into 2% polyvinyl alcohol solution. After 3 h solvent evaporation under mechanical stirring (500 rpm), nanoparticles were collected by centrifugation (15,000 \times g, 30 min, 4°C) and washed thrice with MilliQ water.

2.4.2 MMVs coating

Lyophilized PLGA nanoparticles were combined with MMVs at 1:10 w/w protein:PLGA ratio. Sonication (GuTel GT-100 water bath, 40 kHz, 3 min) generated TGF- β 1-loaded MMV-

nanoparticles (TMNP), which underwent lyophilization (Christ Alpha 2-4 LSCplus, -50°C, 0.05 mBar, and 48 h). MMV-nanoparticles without TGF- β 1 loading (MNP) was defined as control.

2.5 Nanoparticle characterization

Morphological analysis employed transmission electron microscopy (Hitachi HT7800) with uranyl acetate negative staining. Hydrodynamic diameter and zeta potential were determined via dynamic light scattering (Malvern Zetasizer) and nanoparticle tracking analysis (ZetaView[®]), respectively. Encapsulation efficiency ($89.7\% \pm 2.4\%$) was calculated as (encapsulated TGF- β 1/total TGF- β 1) \times 100 after DMSO dissolution, while drug-loading capacity ($4.31\% \pm 0.18\%$) represented (encapsulated TGF- β 1/TMNP mass) \times 100, both quantified by enzyme linked immunosorbent assay (ELISA). Stability assessments monitored hydrodynamic diameter at 4°C over 7 days and turbidity at 560 nm. Release kinetics in 0.5% Tween-80/PBS (pH7.4) at 37°C demonstrated sustained release >96 h via ELISA quantification.

2.6 VILI protocol

Anesthetized mice (tribromoethanol 20 mg/kg i.p.) underwent orotracheal intubation and mechanical ventilation (SAR-100) under high tidal volume (HTV: 20 mL/kg) or normal tidal volume (NTV: 7 mL/kg) for 4 h. Cohorts ($n = 4$ /group) were euthanized at post-ventilation day 1 (PV1d) and day 10 (PV10d). Sham controls received intubation without ventilation. Bronchoalveolar lavage fluid (BALF) from left lungs, serum, and lung tissue were stored at -80 °C; right upper/middle lobes underwent frozen sectioning and TEM processing.

2.7 Therapeutic administration

TMNP (0.5 mg/kg), MNP (0.5 mg/kg), or free recombinant TGF- β 1 (40 μ g/kg) (16, 17) in 50 μ L saline were administered intravenously pre-ventilation. Vehicle controls received saline alone.

2.8 Pathological assessments

2.8.1 Edema quantification

Lung wet/dry weight ratios were calculated after 48 h desiccation at 60°C.

2.8.2 Inflammation profiling

BALF protein (BCA assay), cellular composition (automated cytometry), and cytokine levels (IL-1 β , IL-6, TNF- α , TGF- β 1; ELISA) were analyzed.

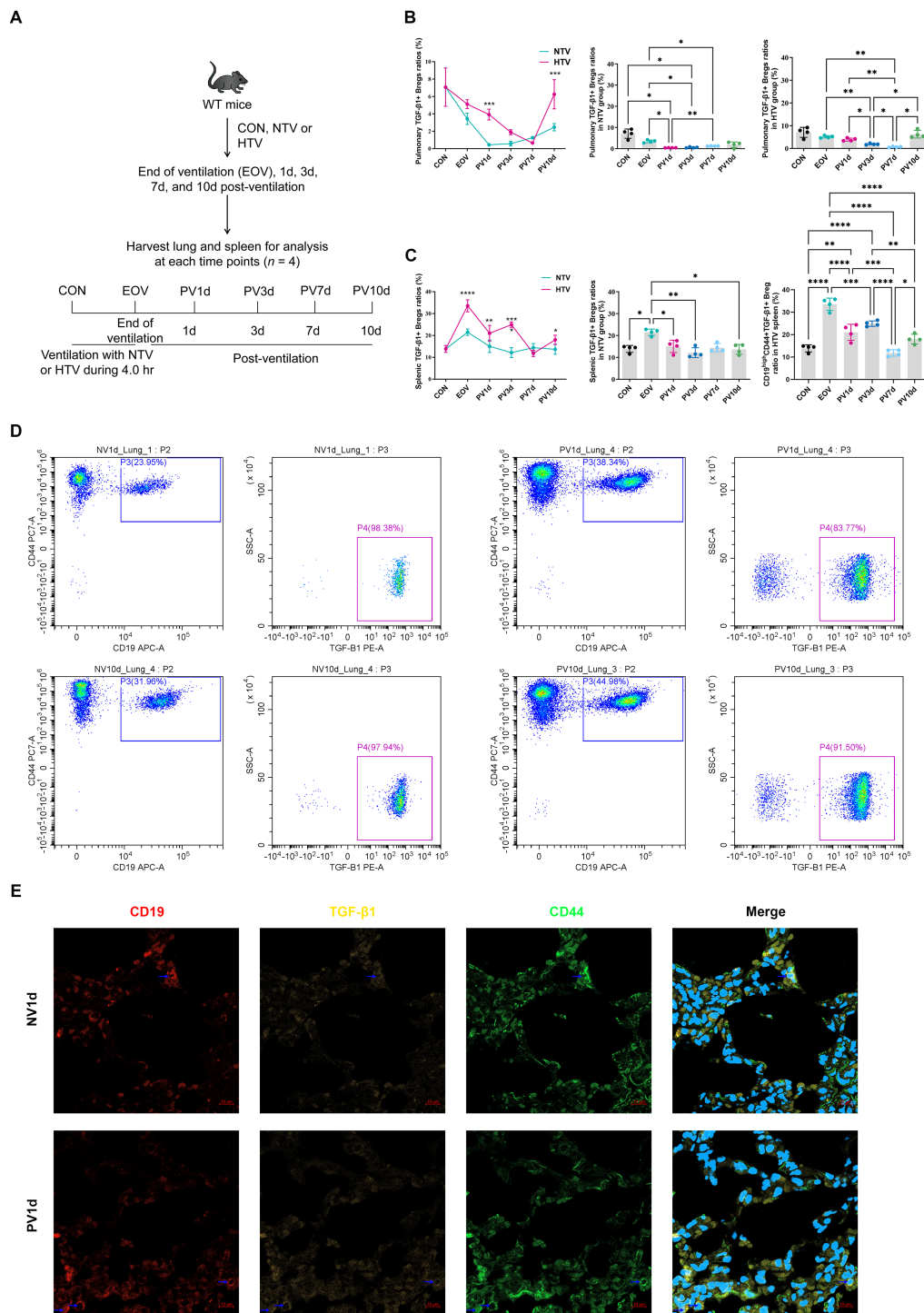


FIGURE 1
 Temporal dynamics of TGF-β1-producing bregs in ventilator-induced lung injury resolution experimental timeline (A) and flow cytometric quantification of pulmonary (B) and splenic (C) TGF-β1+ Breg (pBreg) frequencies following high tidal volume (HTV) or normal tidal volume (NTV) ventilation. Representative flow profiles (D) and confocal microscopy (E) demonstrate enhanced pulmonary Breg infiltration in HTV mice at post-ventilation day 1 (scale: 10 μm). Data represent mean ± SEM (n = 4 mice/group). *P<0.05, **P<0.01, ***P<0.001, ****P<0.0001 vs. NTV controls.

2.8.3 Histopathological evaluation

H&E-stained sections were scored for alveolar hemorrhage, neutrophil infiltration, and hyaline membrane using established criteria (10, 11). Ultrastructural analysis employed TEM (Hitachi HT7800).

2.9 Immunophenotyping

Lung/spleen single-cell suspensions were prepared via enzymatic digestion (0.1 mg/ml Dispase II, 2000 U/ml DNase I,

0.2% collagenase). After Fc receptor blocked (TruStain FcX™ PLUS), cells were stained with fluorochrome-conjugated antibodies (Biolegend/BD Biosciences: CD5-PE, CD19-APC, CD4-FITC, CD8a-APC, CD44-PE/Cy7, LAP-PE) and analyzed by flow cytometry (CytoFLEX LX, Beckman Coulter).

2.10 Multiplex immunofluorescence

Frozen sections underwent fixation (4% paraformaldehyde), permeabilization (0.2% Triton X-100), and blocking (3% BSA/3%

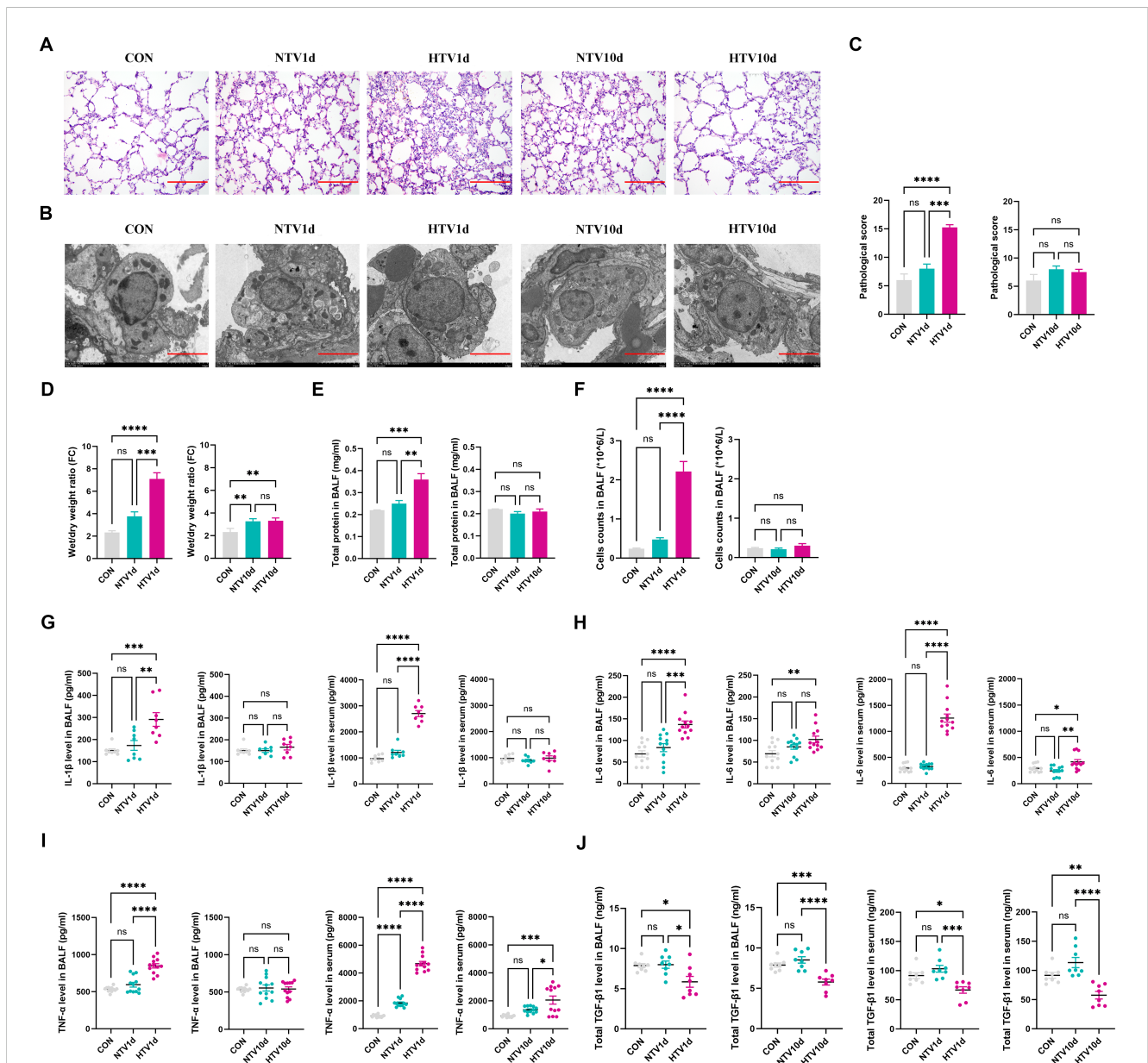


FIGURE 2
Biphasic pathophysiological progression of ventilator-induced lung injury. (A) Histopathological assessment showing alveolar hemorrhage and neutrophil infiltration in H&E-stained sections (A, scale: 100 μm) and ultrastructural alveolar epithelial cell damage by TEM (scale: 5 μm). Quantitative metrics include histopathology scores, lung wet/dry ratios, bronchoalveolar lavage fluid protein/cells, and cytokine levels (C–J) during injury resolution. Data represent mean ± SEM; n = 4. *P<0.05, **P<0.01, ***P<0.001, ****P<0.0001 vs. CON. NTV1d/NTV10d: NTV recovery at 1/10 days; HTV1d/HTV10d: HTV recovery at 1/10 days. Quantitative metrics include histopathology scores, lung wet/dry ratios, bronchoalveolar lavage fluid protein/cell content, and cytokine levels (C–J) during injury resolution. Data represent mean ± SEM (n = 4 mice/group). *P<0.05, **P<0.01, ***P<0.001, ****P<0.0001.

goat serum). Sequential incubations with primary antibodies (anti-CD19, LAP, CD44) and Alexa Fluor-conjugated secondaries preceded DAPI nuclear counterstaining. Imaging utilized a Zeiss LSM980 Airyscan confocal microscope.

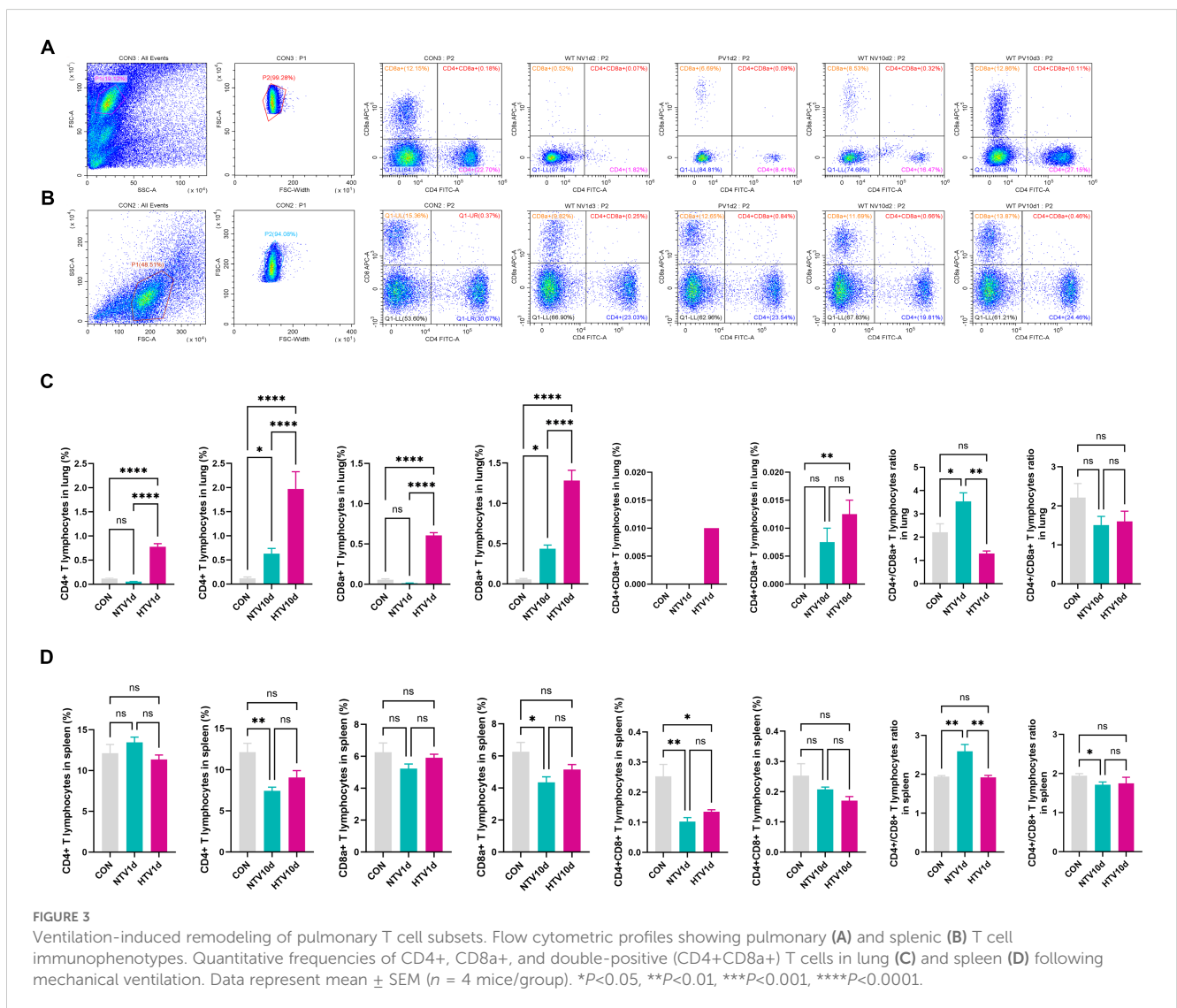
3 Results

3.1 Spatiotemporal dynamics of CD19^{high}CD44^{high}TGF-β1+ Breg in VILI resolution

High-throughput immunophenotyping revealed selective upregulation of tissue migration receptors (CD44, CX3CR1) (18, 19) on splenic Bregs following 4-hour HTV ventilation, while canonical B cell markers remained unchanged (Supplementary Figure S1A). Protein interaction networks demonstrated direct associations between CD19, CD44, and TGF-β1 (Supplementary Figure S1B), with pathway enrichment implicating B cell receptor signaling and epithelial-mesenchymal transition regulation (Supplementary Figures S1C, D).

2.11 Statistical analysis

Bioinformatic analyses employed DAVID (v6.8) for pathway enrichment and STRING (v11.5) for protein interactions (combined score >0.4). Following normality assessment (Shapiro-Wilk), two-tailed t-test (two groups), one-way ANOVA with Tukey's *post-hoc* (multi-group), or two-way ANOVA with Bonferroni correction (time courses) were applied. Data represent mean ± SEM; *P*<0.05 defined statistical significance.



Longitudinal analysis identified a two-phase Breg expansion in lungs: an acute peak at PV1d; 7.83-fold vs. NTV controls: $P < 0.001$) followed by secondary resurgence at PV10d (Figures 1B, D). Conversely, splenic Breg peaked at end-of ventilation (EOV) before declining (Figures 1C, D). Confocal microscopy confirmed enhanced Breg infiltration in HTV-PV1d lungs (Figure 1E), corroborated by flow cytometry (Supplementary Figure S2).

3.2 Time-resolved pathological progression of VILI

HTV-PV1d lungs exhibited hallmark histopathology—alveolar hemorrhage, neutrophil infiltration, and hyaline membranes—alongside ultrastructural damage to alveolar type II epithelial cells (mitochondrial swelling, lamellar body degeneration; Figures 2A, B).

Quantitative metrics peaked at PV1d: lung wet/dry ratio increased 1.98-fold ($P < 0.001$ vs. sham), BALF protein rose 38% ($P < 0.01$), and proinflammatory cytokines (IL-1 β , IL-6/, TNF- α) surged >4-fold ($P < 0.001$, Figures 2C–J). Resolution occurred by PV10d despite persistent TGF- β 1 elevation.

3.3 VILI-associated lymphocyte remodeling

High-resolution immunophenotyping revealed dynamic T cell redistribution in VILI progression (Figures 3A, B). At PV1d, HTV-exposed lungs exhibited significant expansion of both CD4+ (4.3-fold vs CON, $P < 0.0001$) and CD8a+ T cells (6.1-fold vs NTV, $P < 0.0001$), whereas pulmonary CD4+/CD8a+ ratios were elevated in NTV1d versus CON and HTV1d groups ($P < 0.05$).

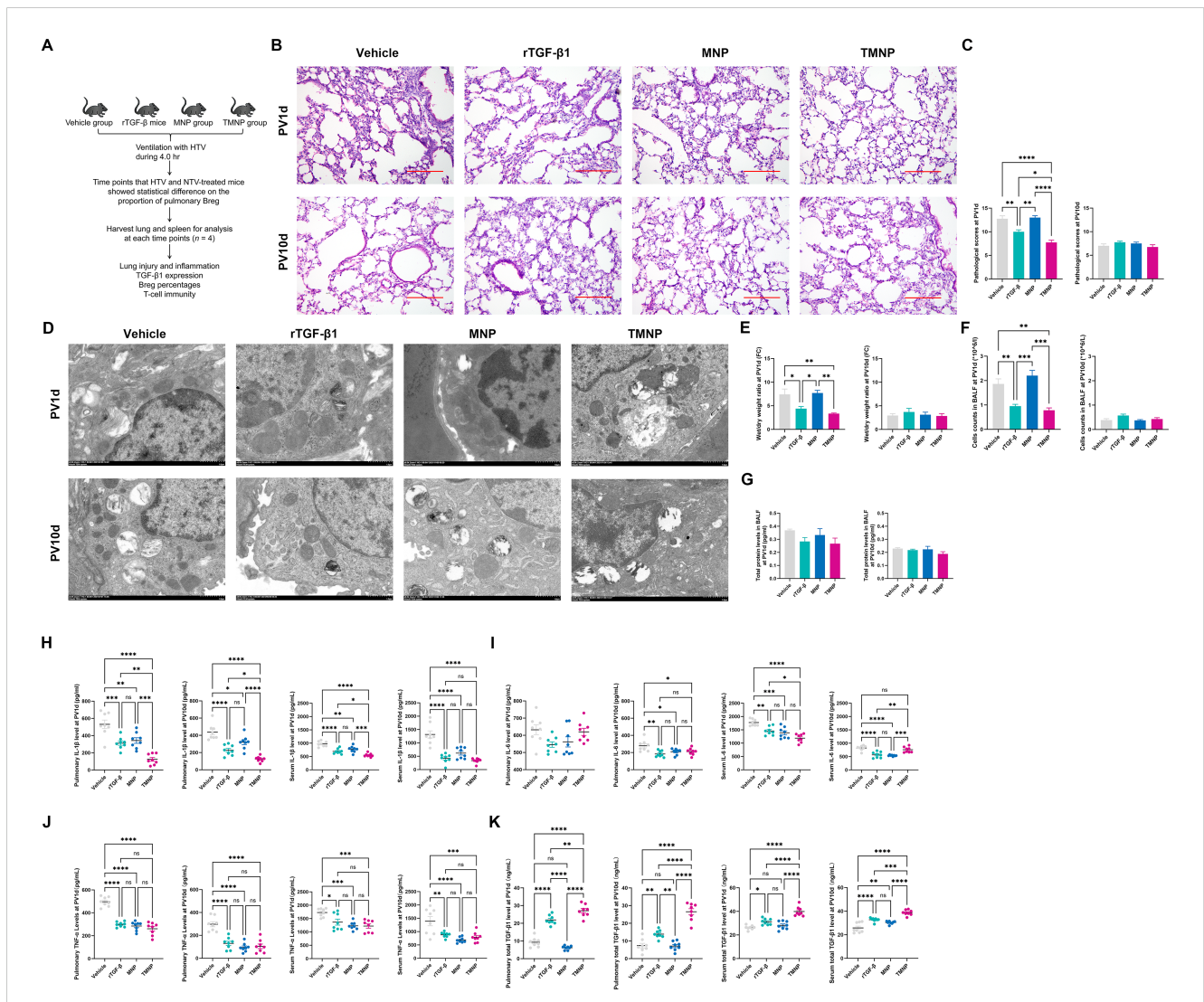


FIGURE 4 Therapeutic Efficacy of TGF- β 1-loaded nanoparticles in Acute lung injury. Administration schema (A) and histological assessment (B, scale: 100 μ m) showing TMNP-mediated protection. Quantitative outcomes include histopathology scores, ultrastructure preservation (TEM scale: 1 μ m), edema reduction, and cytokine modulation (C–K). Data represent mean \pm SEM ($n = 4$ mice/group). * $P < 0.05$, ** $P < 0.01$, *** $P < 0.001$, **** $P < 0.0001$.

Longitudinal analysis demonstrated progressive accumulation of pulmonary CD4+CD8a+ double-positive T cells (DPTCs), with HTV10d showing 9.6-fold increase over CON ($P < 0.01$; **Figure 3C**). Conversely, splenic T cell subsets at PV1d showed no intergroup differences. Notably, both NTV1d and HTV1d cohorts displayed reduced splenic DPTC frequencies (≤ 0.4 -fold vs CON, $P < 0.01$), while NTV1d maintained higher CD4+/CD8a+ ratios than CON and HTV1d ($P < 0.01$).

By PV10d, NTV mice exhibited significant splenic lymphopenia: CD4+ and CD8a+ T cell frequencies decreased 48% and 37% versus CON ($P < 0.01$), respectively, with concomitant reduction in CD4+/CD8a+ ratios (**Figure 3D**).

3.4 Enhanced therapeutic efficacy of TMNP

TMNP demonstrated superior pharmacokinetics: sustained TGF- β 1 release (35.8% EE) and colloidal stability (zeta potential:

-26.7 mV; **Supplementary Figures S3F-H**). In HTV mice, TMNP administration significantly attenuated acute injury at PV1d (histopathology score reduced 22.5% vs. recombinant TGF- β 1; $P < 0.01$; **Figures 4B-F**) while maintaining 3.6-fold higher pulmonary TGF- β 1 levels at PV10d ($P < 0.001$ vs. controls; **Figure 4K**), enabling prolonged immunomodulation.

3.5 TMNP reprograms lymphocyte crosstalk

Single-dose TMNP induced early pulmonary Breg expansion (PV1d: 2.66-fold vs. vehicle; $P < 0.001$; **Figures 5A, C**) and late-phase splenic Breg polarization (PV10d: 59.7% increase vs. recombinant TGF- β 1; $P < 0.01$; **Figures 5B, C**). This coordinated response drove dynamic T cell remodeling: TMNP suppressed pulmonary CD4+ T cells (PV10d: 5.75 fold reduction vs. MNP; $P < 0.05$) while expanding CD8a+ and double-positive T cells (DPTC; **Figures 6A-D**).

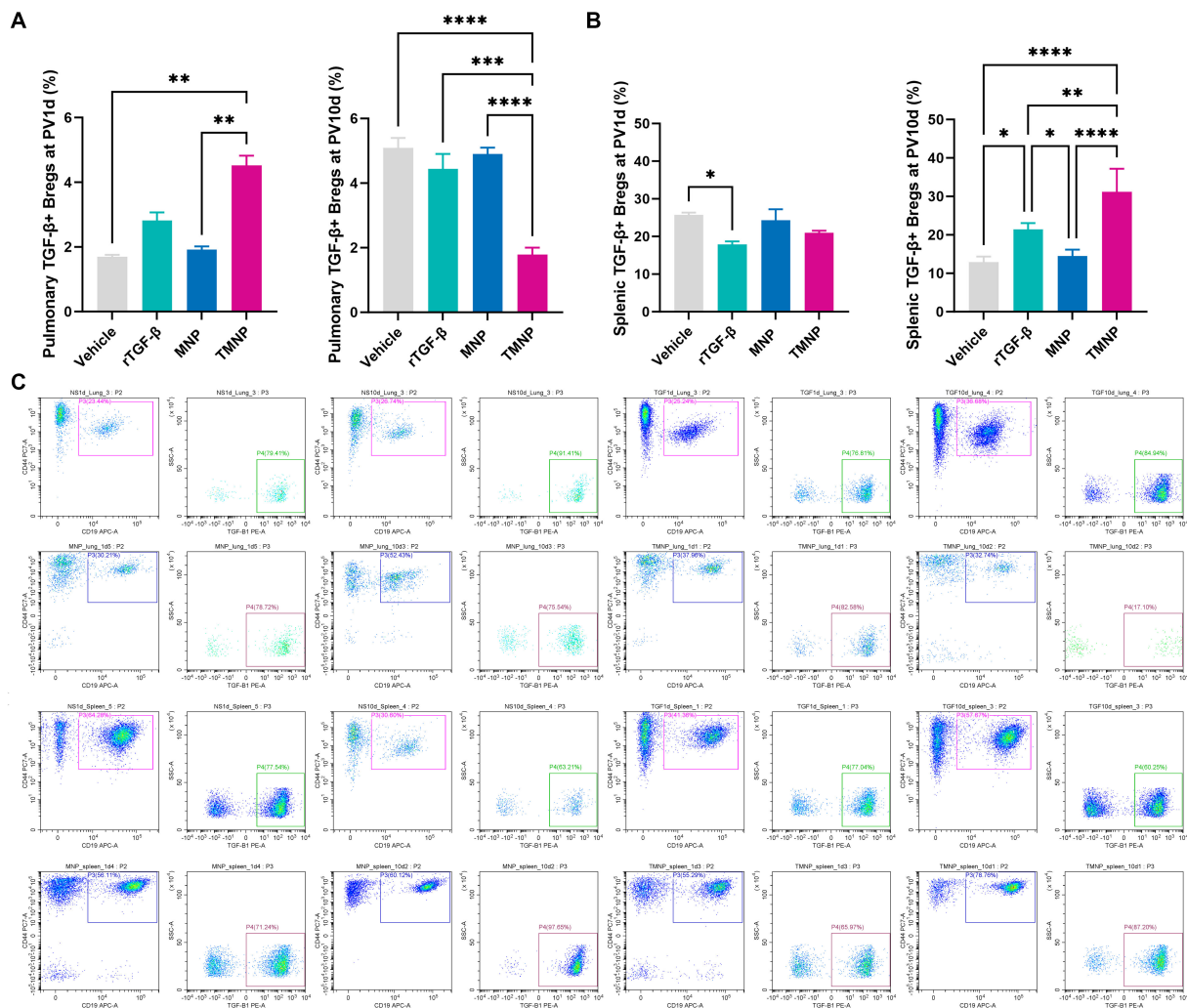


FIGURE 5 Spatiotemporal regulation of breg populations by nanoparticle therapy. Flow cytometric quantification demonstrating pulmonary (A) and splenic (B) Breg expansion following TMNP administration. Representative gating profiles illustrate subset dynamics (C). Data represent mean \pm SEM ($n = 4$ mice/group). * $P < 0.05$, ** $P < 0.01$, *** $P < 0.001$, **** $P < 0.0001$.

Multivariate analysis revealed splenic Breg-CD4+CD8a+ T cell antagonism ($r=0.559$; **Supplementary Figure S4B**) and TGF- β 1-mediated IL-6 suppression ($r=-0.444$; **Supplementary Figure S4A**).

4 Discussion

Our study establishes CD19^{high}CD44^{high}TGF- β 1+ Bregs as spatiotemporal orchestrators of VILI resolution, with their therapeutic potential unlocked through biomimetic nanoparticle delivery. Building on previous work demonstrating IL-10+ Bregs involvement in chronic inflammation (20–22), we reveal TGF- β 1+ Bregs exhibit phased activation: an acute pulmonary influx at PV1d to contain neutrophil extracellular traps (23, 24), followed by splenic priming atPV10d regulating CD4+CD8a+ T cell-mediated immunosuppression. This mirrors their dual role in cancer immunity—restraining early inflammation while permitting late-phase tolerance (25).

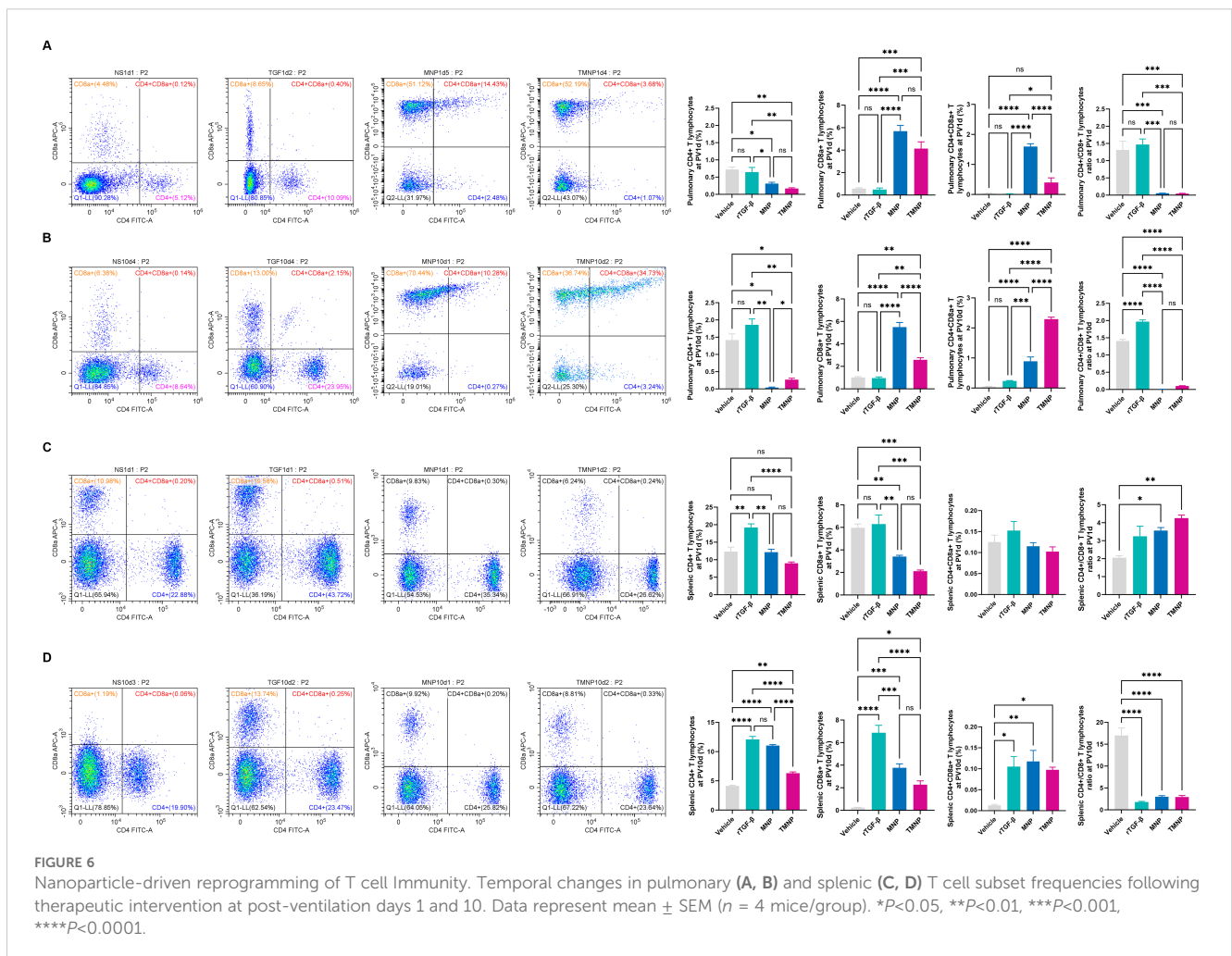
Nanotechnology-driven cytokine precision represents a transformative advance over conventional TGF- β 1 therapy, which fails clinically due to pleiotropic effects and transient bioavailability

(14). TMNP overcome these limitations through pH-responsive sustained release (>72 h vs. recombinant TGF- β 1's 6 h peak) (26) and Flotillin-2-mediated alveolar macrophage targeting (27). This aligns with emerging nanotherapeutic strategies for ARDS while demonstrating superior spatiotemporal control (28, 29).

We further identify CD4+CD8a+ T cells as TGF- β 1+ Breg-regulated effectors in lung repair. Their expansion correlates inversely with splenic Breg activity ($r=-0.72$, $P < 0.01$) and parallels tumor-associated CD4+CD8a+ T cells that modulate CD8+ T cells via TGF- β 1/PD-1 signaling (30), suggesting conserved immunosuppressive mechanisms across inflammatory contexts.

5 Clinical implications & limitations

While TMNP show compelling efficacy in acute inflammation, key questions require resolution: First, whether CD4+CD8a+ T cell expansion predispose to post-VILI fibrosis merits investigation using lineage-tracing models. Second, MMV coatings should be engineered to avoid tumor-promoting Breg phenotypes observed in cancer models (31). Crucially, human relevance must be established through humanized mouse systems—for example, NSG mice



reconstituted with human hematopoietic stem cells could validate Breg dynamics across ventilation injury phases.

6 Concluding perspective

This work provides the first temporal mapping of TGF- β 1+ Bregs in VILI, linking acute pulmonary infiltration to late splenic regulation of CD4+CD8a+ T cell interactions. Our MMV-based nanoformulation enables dual-phase immunomodulation: rapid injury containment and sustained homeostasis. By redefining CD4+CD8a+ T cell as key effectors in lung repair and demonstrating nanotechnology-enhanced cytokine delivery, we established a template for biomimetic therapeutics in ARDS management. Future studies should explore adoptive Breg transfer and cell-specific Tgfb1 deletion models to establish causal mechanisms.

Data availability statement

The original contributions presented in the study are included in the article/Supplementary Material. Further inquiries can be directed to the corresponding author.

Ethics statement

The animal study was approved by Male C57BL/6 mice (4–6 weeks, 25 \pm 5 g) were sourced from the Animal Center of Guangxi Medical University (Nanning, China). All procedures adhered to China's Laboratory Animal Welfare Guidelines under IACUC protocol KY-2022-288. The study was conducted in accordance with the local legislation and institutional requirements.

Author contributions

RJ: Project administration, Methodology, Formal analysis, Data curation, Writing – original draft. XL: Data curation, Formal analysis, Methodology, Project administration, Resources, Writing – review & editing. JM: Software, Writing – review & editing, Formal analysis, Data curation, Methodology. SH: Software, Formal analysis, Writing – review & editing, Methodology, Data curation. XX: Investigation, Writing – review & editing, Project administration, Methodology, Data curation. ZH: Writing – review & editing, Resources, Data curation, Methodology, Formal analysis. LP: Validation, Investigation, Writing – review & editing, Conceptualization, Funding acquisition, Supervision, Visualization.

Funding

The author(s) declare that financial support was received for the research and/or publication of this article. This work was supported

by grants from the National Natural Science Foundation of China (81970078), Guangxi Anesthesiology Clinical Medicine Research Center Construction Project (scientific foundation of Guangxi No: 2022AC04002), Youth Science Foundation of Guangxi Medical University (GXMUYSF202120), and Innovation Project of Guangxi Graduate Education (YCBZ2021043).

Conflict of interest

The authors declare that the research was conducted in the absence of any commercial or financial relationships that could be construed as a potential conflict of interest.

Generative AI statement

The author(s) declare that no Generative AI was used in the creation of this manuscript.

Publisher's note

All claims expressed in this article are solely those of the authors and do not necessarily represent those of their affiliated organizations, or those of the publisher, the editors and the reviewers. Any product that may be evaluated in this article, or claim that may be made by its manufacturer, is not guaranteed or endorsed by the publisher.

Supplementary material

The Supplementary Material for this article can be found online at: <https://www.frontiersin.org/articles/10.3389/fimmu.2025.1635178/full#supplementary-material>

SUPPLEMENTARY FIGURE 1

Molecular Signatures of TGF- β 1+ Bregs in Ventilator-Induced Lung Injury. Flow gating strategy (A), protein-protein interaction network (B), and pathway enrichment analysis (C, D) characterizing regulatory B cell populations.

SUPPLEMENTARY FIGURE 2

Splenic Breg Dynamics during Injury Progression. Gating hierarchy (A) and quantitative frequencies (B, C) of splenic Breg subpopulations at end-of-ventilation and recovery timepoints ($n = 4$ mice/group).

SUPPLEMENTARY FIGURE 3

Biophysical Characterization of Macrophage-Mimetic Nanoparticles. Microvesicle biogenesis (A, B, scale: 20 μ m), membrane protein validation (C, D), electron microscopy (E, scale: 100 nm), colloidal stability (F, G), sustained cytokine release profile (H), and serum compatibility (I) of engineered nanotherapeutics.

SUPPLEMENTARY FIGURE 4

Systems-Level Correlation Networks in Lung Pathobiology. Pearson correlations matrices showing TGF- β 1-IL-6 axis regulation (A), Breg-T cell interactions (B–D), lymphocyte subset interplay (E–G), and biomarker relationships (H–J). * $P < 0.05$ after Bonferroni correction.

References

- Wick KD, Ware LB, Matthay MA. Acute respiratory distress syndrome. *Bmj*. (2024) 387:e076612. doi: 10.1136/bmj-2023-076612
- Perez-Fernandez XL, Sabater-Riera J, Fuset-Cabanes M. COVID-19 ARDS: getting ventilation right. *Lancet*. (2022) 399:22. doi: 10.1016/S0140-6736(21)02439-9
- Albert RK. Constant vt ventilation and surfactant dysfunction: an overlooked cause of ventilator-induced lung injury. *Am J Respir Crit Care Med*. (2022) 205:152–60. doi: 10.1164/rccm.202107-1690CP
- Gama de Abreu M, Sessler DI. Mechanical power: correlate or cause of ventilator-induced lung injury? *Anesthesiology*. (2022) 137:6–8. doi: 10.1097/ALN.0000000000004240
- Cherukuri A, Mohib K, Rothstein DM. Regulatory B cells: TIM-1, transplant tolerance, and rejection. *Immunol Rev*. (2021) 299:31–44. doi: 10.1111/imr.12933
- Menon M, Hussell T, Ali Shuha H. Regulatory B cells in respiratory health and diseases. *Immunol Rev*. (2021) 299:61–73. doi: 10.1111/imr.12941
- Manfroi B, Fillatreau S. Regulatory B cells gain muscles with a leucine-rich diet. *Immunity*. (2022) 55:970–2. doi: 10.1016/j.immuni.2022.05.011
- Wang L, Christodoulou MI, Jin Z, Ma Y, Hossen M, Ji Y, et al. Human regulatory B cells suppress autoimmune disease primarily via interleukin-37. *J Autoimmun*. (2025) 153:103415. doi: 10.1016/j.jaut.2025.103415
- Bao Y, Liu J, Li Z, Sun Y, Chen J, Ma Y, et al. Ex vivo-generated human CD1c(+) regulatory B cells by a chemically defined system suppress immune responses and alleviate graft-versus-host disease. *Mol Ther*. (2024) 32:4372–82. doi: 10.1016/j.yimthe.2024.10.026
- Jing R, He S, Liao XT, Xie XL, Mo JL, Hu ZK, et al. Transforming growth factor- β 1 attenuates inflammation and lung injury with regulating immune function in ventilator-induced lung injury mice. *Int Immunopharmacol*. (2023) 114:109462. doi: 10.1016/j.intimp.2022.109462
- Jing R, Xie X, Liao X, He S, Mo J, Dai H, et al. Transforming growth factor- β 1 is associated with inflammatory resolution via regulating macrophage polarization in lung injury model mice. *Int Immunopharmacol*. (2024) 142:112997. doi: 10.1016/j.intimp.2024.112997
- Huang LT, Chou HC, Chen CM. Inhibition of FABP4 attenuates hyperoxia-induced lung injury and fibrosis via inhibiting TGF- β signaling in neonatal rats. *J Cell Physiol*. (2022) 237:1509–20. doi: 10.1002/jcp.30622
- Isabel FC, Carlos MS. “TGF β 1 (Transforming Growth Factor, Beta 1)”. In: 2nd ed. John Libbey Eurotext. *Atlas of Genetics and Cytogenetics in Oncology and Haematology*. (2013). p. 655–668. Available online at: <https://atlasgeneticsoncology.org/gene/451/TGFB1>.
- Li M, Zeng L, Liu S, Dangelmajer S, Kahlert UD, Huang H, et al. Transforming growth factor- β Promotes homing and therapeutic efficacy of human mesenchymal stem cells to glioblastoma. *J Neuropathol Exp Neurol*. (2019) 78:315–25. doi: 10.1093/jnen/nlz016
- Li R, He Y, Zhu Y, Jiang L, Zhang S, Qin J, et al. Route to rheumatoid arthritis by macrophage-derived microvesicle-coated nanoparticles. *Nano Lett*. (2019) 19:124–34. doi: 10.1021/acs.nanolett.8b03439
- Zhang XY, Liu ZM, Zhang HF, Li YS, Wen SH, Shen JT, et al. TGF- β 1 improves mucosal IgA dysfunction and dysbiosis following intestinal ischaemia-reperfusion in mice. *J Cell Mol Med*. (2016) 20:1014–23. doi: 10.1111/jcmm.12789
- Taylor RA, Chang CF, Goods BA, Hammond MD, Mac Grory B, Ai Y, et al. TGF- β 1 modulates microglial phenotype and promotes recovery after intracerebral hemorrhage. *J Clin Invest*. (2017) 127:280–92. doi: 10.1172/JCI88647
- Greiffo FR, Viteri-Alvarez V, Frankenberger M, Dietel D, Ortega-Gomez A, Lee JS, et al. CX3CR1-fractalkine axis drives kinetic changes of monocytes in fibrotic interstitial lung diseases. *Eur Respir J*. (2020) 55(2):1900460. doi: 10.1183/13993003.00460-2019
- Klement JD, Paschall AV, Redd PS, Ibrahim ML, Lu C, Yang D, et al. An osteopontin/CD44 immune checkpoint controls CD8+ T cell activation and tumor immune evasion. *J Clin Invest*. (2018) 128:5549–60. doi: 10.1172/JCI123360
- Garcia-Lacarte M, Grijalba SC, Melchor J, Pascual M, Goñi E, Clemente-Larramendi I, et al. IL-10 from tumoral B cells modulates the diffuse large B-cell lymphoma microenvironment and response to immunotherapy. *Blood*. (2025) 145:2746–61. doi: 10.1182/blood.2024025755
- Hua F, Sun L, Li Y, Meng Y, Fan X, Wang X, et al. CD19(+)IL-10(+) regulatory B cells induced by IL-12p35 regulates functional T-cell subsets in patients with immune thrombocytopenia. *Br J Haematol*. (2025). doi: 10.1111/bjh.20173
- Hertz D, Marwitz S, Eggers L, von Borstel L, Harikumar Parvathy G, Behrends J, et al. Sex-specific impact of B cell-derived IL-10 on tuberculosis resistance. *Front Immunol*. (2025) 16:1524500. doi: 10.3389/fimmu.2025.1524500
- Lee W, Ko SY, Akasaka H, Weigert M, Lengyel E, Naora H. Neutrophil extracellular traps promote pre-metastatic niche formation in the omentum by expanding innate-like B cells that express IL-10. *Cancer Cell*. (2025) 43:69–85.e11. doi: 10.1016/j.ccell.2024.12.004
- Crowley LE, Stockley RA, Thickett DR, Dosanjh D, Scott A, Parekh D. Neutrophil dynamics in pulmonary fibrosis: pathophysiological and therapeutic perspectives. *Eur Respir Rev*. (2024) 33(174):240139. doi: 10.1183/16000617.0139-2024
- Michee-Cospolite M, Boudigou M, Grasseau A, Simon Q, Mignen O, Pers JO, et al. Molecular mechanisms driving IL-10- producing B cells functions: STAT3 and c-MAF as underestimated central key regulators? *Front Immunol*. (2022) 13:818814. doi: 10.3389/fimmu.2022.818814
- Yao Y, Fan S, Fan Y, Shen X, Chai X, Shao Y, et al. Intratracheal delivery of macrophage targeted Celastrol-loaded PLGA nanoparticles for enhanced anti-inflammatory efficacy in acute lung injury mice. *Eur J Pharm Biopharm*. (2024) 204:114511. doi: 10.1016/j.ejpb.2024.114511
- Mishra S, Liao W, Liu Y, Yang M, Ma C, Wu H, et al. TGF- β and Eomes control the homeostasis of CD8+ regulatory T cells. *J Exp Med*. (2021) 218(1):e20200030. doi: 10.1084/jem.20200030
- Zhang HH, Kuo WS, Tu PY, Lee CT, Wang HC, Huang YT, et al. Enhancing lung recovery: inhaled poly(lactic-co-glycolic) acid encapsulating FTY720 and nobiletin for lipopolysaccharide-induced lung injury, with advanced inhalation tower technology. *ACS Nano*. (2025) 19:7634–49. doi: 10.1021/acsnano.3c12532
- Wang Y, Zhang LF, Zhang JJ, Yu SS, Li WL, Zhou TJ, et al. Spontaneous inflammation resolution inspired nanoparticles promote neutrophil apoptosis and macrophage efferocytosis for acute respiratory distress syndrome treatment. *Adv Healthc Mater*. (2025) 14:e2402421. doi: 10.1002/adhm.202402421
- Maher AK, Aristodemou A, Giang N, Tanaka Y, Bangham CR, Taylor GP, et al. HTLV-1 induces an inflammatory CD4+CD8+ T cell population in HTLV-1-associated myelopathy. *JCI Insight*. (2024) 9(1):e173738. doi: 10.1172/jci.insight.173738
- Wang Z, Zhou Y, Yu Y, He K, Cheng LM. Lipopolysaccharide preconditioning increased the level of regulatory B cells in the spleen after acute ischaemia/reperfusion in mice. *Brain Res*. (2018) 1701:46–57. doi: 10.1016/j.brainres.2018.05.036